

1 **Characterizing microRNA-mediated modulation of gene expression**
2 **noise and its effect on synthetic gene circuits**

3 Lei Wei^{1¶}, Shuailin Li^{2¶}, Tao Hu¹, Michael Q. Zhang^{1,3,4}, Zhen Xie¹, Xiaowo Wang^{1,*}

4 ¹ MOE Key Laboratory of Bioinformatics; Bioinformatics Division and Center for Synthetic & Systems Biology,
5 Beijing National Research Center for Information Science and Technology; Department of Automation, Tsinghua
6 University, Beijing 100084, China

7 ² School of Life Sciences, Tsinghua University, Beijing 100084, China

8 ³ Department of Basic Medical Sciences, School of Medicine, Tsinghua University, Beijing 100084, China

9 ⁴ Department of Biological Sciences, Center for Systems Biology, University of Texas at Dallas, Dallas 800 West
10 Campbell Road, RL11, Richardson, TX 75080-3021, USA

11

12 * Correspondence: xwwang@tsinghua.edu.cn

13 ¶ These authors contributed equally to this work.

14

15 **Keywords:** gene expression noise; miRNA; competing RNA; competition; synthetic
16 gene circuits

17

1 **Abstract**

2 Gene expression noise plays an important role in many biological processes, such as
3 cell differentiation and reprogramming. It can also dramatically influence the behavior
4 of synthetic gene circuits. MicroRNAs (miRNAs) have been shown to reduce the noise
5 of lowly expressed genes and increase the noise of highly expressed genes, but less is
6 known about how miRNAs with different properties may regulate gene expression
7 noise differently. Here, by quantifying gene expression noise using mathematical
8 modeling and experimental measurements, we showed that competing RNAs and the
9 composition of miRNA response elements (MREs) play important roles in modulating
10 gene expression noise. We found that genes targeted by miRNAs with weak competing
11 RNAs show lower noise than those targeted by miRNAs with strong competing RNAs.
12 In addition, in comparison with a single MRE, repetitive MREs targeted by the same
13 miRNA suppress the noise of lowly expressed genes but increase the noise of highly
14 expressed genes. Additionally, MREs composed of different miRNA targets could
15 cause similar repression levels but lower noise compared with repetitive MREs. We
16 further observed the influence of miRNA-mediated noise modulation in synthetic gene
17 circuits which could be applied to classify cell types using miRNAs as sensors. We
18 found that miRNA sensors that introduce higher noise could lead to better classification
19 performance. Our results provide a systematic and quantitative understanding of the
20 function of miRNAs in controlling gene expression noise and how we can utilize
21 miRNAs to modulate the behavior of synthetic gene circuits.

22

23 **Introduction**

24 Stochastic fluctuations lead to variation, or noise, in gene expression levels, which is
25 inevitable even among genetically identical cells exposed to the same environmental
26 conditions (1). In clonal populations of microbes, gene expression noise enables cells

1 to generate diverse phenotypes, which may improve the fitness of the population in
2 certain environments (2–5). In multicellular organisms, noise is involved in many
3 biological processes, such as cell differentiation (6, 7), reprogramming (8), and
4 apoptosis (9). Noise can give rise to the heterogeneity of cancer cells within individual
5 tumors (10, 11). In addition, gene expression noise can influence the behavior of
6 synthetic gene circuits. In transcriptional cascades, noise is amplified near the transition
7 region of the dose-response curve, reducing the precision of signal transduction (12–
8 15). Nonetheless, noise is necessary in excitable circuits for the initiation of transient
9 state switching (3, 4, 16). Therefore, it is valuable to understand the mechanism of noise
10 modulation in nature and thus to manipulate gene expression noise to control
11 phenotypes according to expectations.

12 MiRNAs are ~22 nt noncoding RNAs that mediate the posttranscriptional regulation of
13 their target genes by either translational repression or poly(A)-tail shortening (17, 18).
14 Recently, researchers proposed that miRNAs can control gene expression noise and
15 confer robustness to biological processes (19–23). MiRNAs can reduce the noise of
16 lowly expressed genes by accelerating mRNA turnover, which can be compensated for
17 by higher transcription rates, and miRNAs can increase the noise of highly expressed
18 genes by introducing additional extrinsic noise (20). These discoveries provided an
19 explanation for the observation that many highly expressed housekeeping genes do not
20 harbor miRNA binding sites (24). Furthermore, the capacity of miRNAs to modulate
21 noise was found to be highly related to the strength of their repression on the expression
22 of target genes (20).

23 MiRNAs are important regulators in both natural gene networks and synthetic gene
24 circuits. Different types of miRNAs and various miRNA targets are involved in diverse
25 biological processes. Therefore, it is essential to delineate how the properties of
26 miRNAs and their targets beyond repression strength, such as the competing RNAs of
27 miRNAs and the composition of miRNA binding sites, could modulate gene expression

1 noise. For example, the competing RNAs of miRNAs have been shown to have the
2 capacity to modulate gene expression noise (25, 26). Previously, we analyzed gene
3 expression noise at the mRNA level by single-cell RNA-seq and revealed that miRNAs
4 with weakly-interacted competing RNAs could buffer gene expression noise compared
5 to miRNAs with few targets (27). However, there is a lack of comprehensive studies to
6 systematically and quantitatively depict how the properties of miRNAs and the
7 compositions of miRNA response elements (MREs) modulate gene expression noise
8 and how such noise modulation further influences the output behavior of synthetic gene
9 circuits. The absence of investigation hinders the understanding and utilization of
10 miRNAs to control gene expression noise in natural gene regulatory networks and
11 synthetic gene circuits.

12 Here, by quantifying gene expression noise via mathematical modeling and flow
13 cytometry analysis with a dual-fluorescent reporter system, we investigated how
14 competing RNA networks can influence gene expression noise at the protein level.
15 Specifically, in comparison with genes targeted by miRNAs with strong competing
16 RNAs, those targeted by miRNAs with weak competing RNAs show reduced gene
17 expression noise over a wide range of gene expression levels. Furthermore, genes with
18 repetitive MREs for the same miRNA exhibit lower noise than genes with a single MRE
19 when the gene expression level is low but show a strong increase in noise when the
20 gene expression level is high due to the saturation effect. Additionally, in comparison
21 with repetitive MREs, MREs composed of targets that are regulated by different
22 miRNAs exert a similar repression strength but cause lower noise on their target genes.
23 To investigate how gene expression noise can influence the behavior of synthetic gene
24 circuits, we further applied the results to a transcription activator-like effector repressor
25 (TALER) switch circuit that can be employed to classify cell types using endogenous
26 miRNAs as sensors. We found that the increase in noise mediated by miRNAs could
27 significantly improve the classification accuracy by enhancing cell state transition. In
28 summary, this work quantitatively characterized patterns of the miRNA-mediated

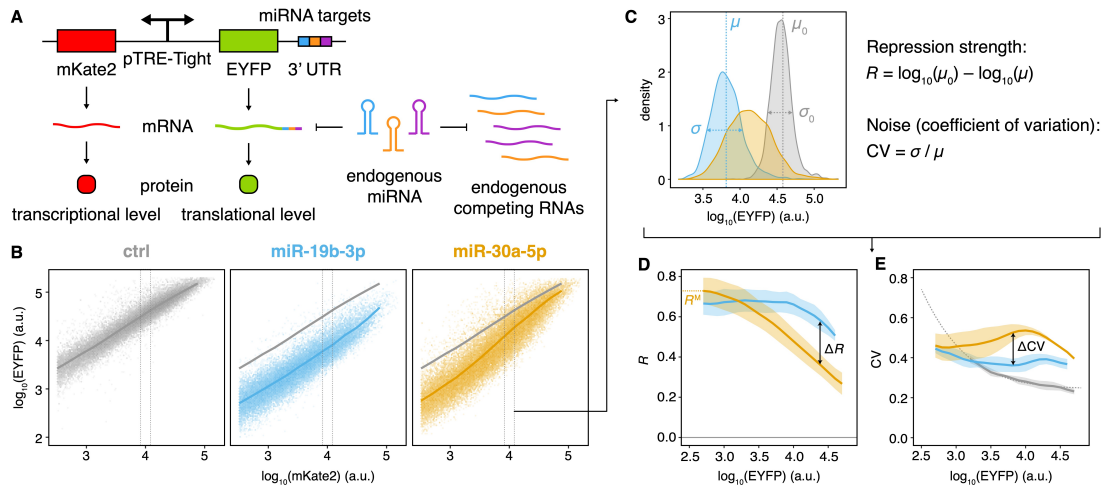
1 modulation of gene expression noise as well as how such modulation influences the
2 performance of synthetic gene circuits. The results provide novel insight into the
3 function of miRNAs in gene regulatory networks and could be useful to guide the
4 design of synthetic gene circuits to confer robustness or variability.

5

6 **Results**

7 **Measurement of gene expression noise by a dual-fluorescent reporter system**

8 To quantify the modulation of gene expression noise by endogenous miRNAs, we
9 constructed a dual-fluorescent reporter system to measure the expression levels and
10 noise of fluorescent proteins in HeLa cells. The system is composed of two fluorescent
11 proteins (mKate2 and EYFP) that are transcribed from a bidirectional promoter. MREs
12 are fused to the 3' untranslated region (3'UTR) of EYFP, whereas the expression of
13 mKate2 is not regulated by miRNAs (Fig. 1A). Therefore, the fluorescence intensity of
14 mKate2 can be used to indicate the transcription rate of the promoter. After the transient
15 transfection of the system into HeLa cells, the intensity of mKate2 and EYFP was
16 quantified by flow cytometry (Fig. 1B). Cells with similar transcription rates were
17 binned according to their mKate2 fluorescence intensity (Fig. 1B). The mean value and
18 noise (coefficient of variation, CV) of the EYFP fluorescence intensity in each bin were
19 calculated (Fig. 1C-E).



1

2 Fig. 1. Measurement of gene expression noise by a dual-fluorescent reporter system.

3 (A) Schematic diagrams of the dual-fluorescent reporter system.

4 (B-E) Procedures for calculating gene expression noise using flow cytometry data. Flow cytometry
5 results of systems with no MRE (gray), the single miR-19b-3p MRE (blue), or the single miR-30a-

6 5p MRE (orange) are shown in (B). Cells were binned according to mKate2 fluorescent intensity

7 (C). The repression strength of miRNAs (D) and the gene expression noise (E) in each bin were

8 further calculated. The lines represent the mean value of EYFP in different mKate2 bins in (B). The

9 lines and shading show the mean \pm SD of three independent replicates in (D) and (E). The dotted

10 line in (E) represents the fitted noise of reporters without MREs.

11 We identified the 20 endogenous miRNAs showing the highest expression in HeLa cells

12 by high-throughput sequencing and cloned one perfectly complementary MRE to the

13 3'UTR of EYFP for each of them (Fig. S1 and Table S1). Then, we measured the

14 correlation between the strength of miRNA-mediated repression (R , logarithmic fold

15 change) and the noise of EYFP (CV) at different EYFP levels (Fig. 2A and Fig. S2).

16 Previous studies (20) have demonstrated that the repression strength of miRNAs is a

17 critical factor in miRNA-mediated noise control. Higher repression strength could

18 reduce intrinsic noise, which is mainly contributed by the stochastic gene transcription,

19 to a greater extent, thus leading to significant noise reduction at low gene expression

20 levels. Additionally, the noise of miRNAs can propagate to the noise of the observed

21 gene as extrinsic noise, which is dominant at high expression levels. Consistent with

1 these findings, we found that miRNA-mediated repression strength was negatively
2 correlated with the noise of EYFP when expressed at a low level but positively
3 correlated under high expression (Fig. 2A). However, the correlation was not
4 sufficiently high when gene expression levels were intermediate. Genes that are
5 repressed to a similar extent may show quite different noise levels (Fig. 2A), leading to
6 the speculation that other properties of miRNAs can also influence gene expression
7 noise.

8

9 **Competing RNAs of miRNAs modulate gene expression noise**

10 It has been shown that each miRNA targets tens or hundreds of different endogenous
11 RNAs (28), yet most of them are only modestly repressed (less than twofold) (29–31).
12 These RNAs compete for miRNA binding with each other, mutually playing the role of
13 competing RNAs and constituting a complex miRNA-mediated regulatory network. By
14 combining mathematical modeling and single-cell RNA-seq analysis, we previously
15 showed that the abundant weak targets of miRNAs have the capacity to buffer gene
16 expression noise (26, 27). In addition, previous research using a similar dual-
17 fluorescent reporter system investigated how the strength of exogenous competing
18 RNAs introduced by transfected plasmids influences gene expression noise (25).
19 However, the binding affinities of these exogenous competing RNAs to miRNAs are
20 much higher than those of endogenous interactions, so the results can hardly represent
21 how endogenous miRNA-mediated regulatory networks modulate gene expression
22 noise.

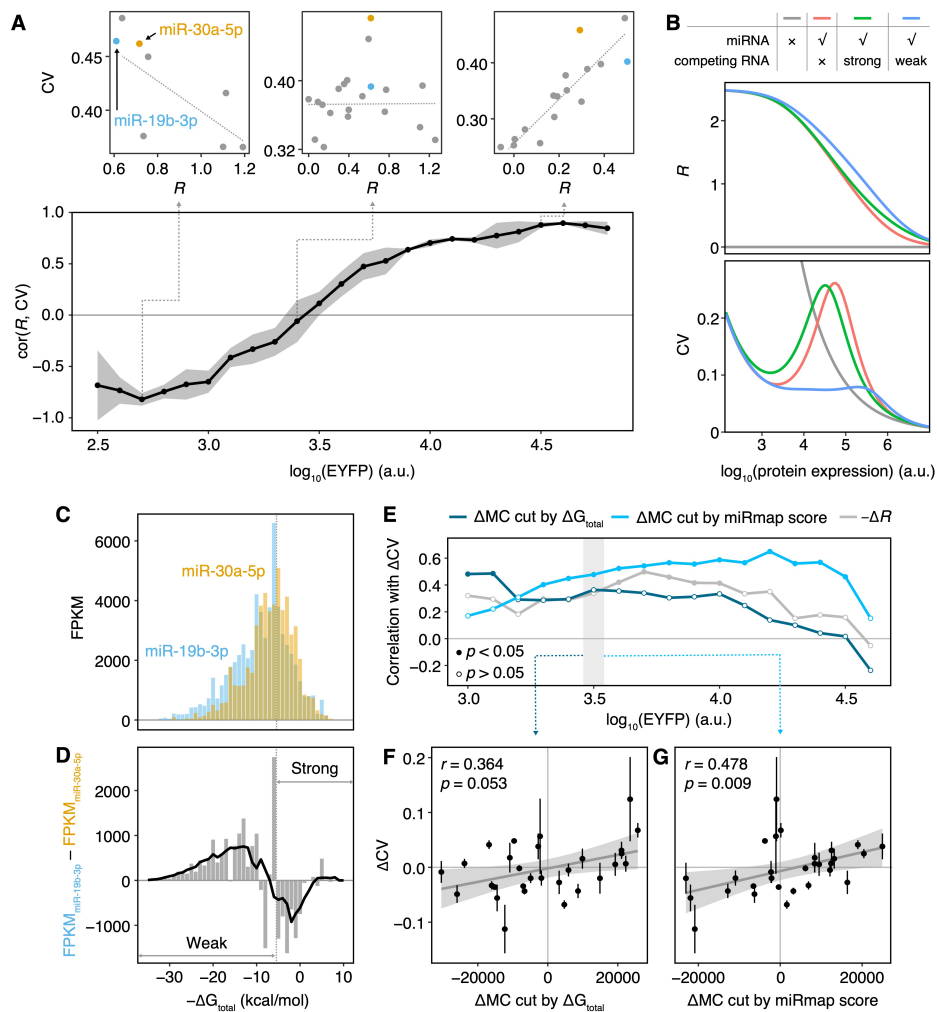
23 To investigate how competing RNAs regulate gene expression noise, we performed
24 computational simulations using a minimal miRNA-competing RNA model that we and
25 others have used previously (26, 32, 33). The model describes the interactions between
26 one miRNA and two RNAs that can bind the miRNA competitively. The simulation

1 results showed that when repression strengths were similar, the noise of lowly
2 expressed genes was not sensitive to competing RNAs. However, at intermediate or
3 high expression levels, genes targeted by miRNAs with weak competing RNA pools
4 tended to show lower noise than genes that were not regulated by any miRNAs and
5 those regulated by miRNAs with strong competing RNA pools (Fig. 2B).

6 To verify the computational results, we used a reporter system to analyze the noise
7 modulation patterns of miRNAs with similar repression ability to exclude the influence
8 of repression strength on noise. As the repression strength may be reduced with the
9 increase of gene expression level (34), we took the repression strength at the lowest
10 EYFP expression level as the maximum repression strength (R^M) to describe the
11 repression ability of a miRNA. To figure out the impact of noise on miRNAs with same
12 repression strength, we chose all miRNA pairs exhibiting a difference of maximum
13 repression strength (ΔR^M , $R^M_{\text{miR-A}} - R^M_{\text{miR-B}}$) less than 0.1 for further analysis. For
14 example, reporters with a single perfectly complementary MRE of miR-30a-5p or miR-
15 19b-3p showed similar repression strengths and noise levels at low expression (Fig.
16 1D). However, at high expression, the reporter with the miR-19b-3p MRE showed less
17 noise than that with the miR-30a-5p MRE (Fig. 1E). We further quantified the levels of
18 the competing RNAs of these miRNAs by RNA-seq and used the total system energy
19 (ΔG_{total}) calculated by miRmap (35) to represent the interaction strength between
20 miRNAs and their competing RNAs. In comparison with miR-19b-3p, miR-30a-5p
21 tended to be associated with more substantial levels of strong competing RNAs and
22 lower levels of weak competing RNAs (Fig. 2C-D). Therefore, consistent with the
23 computational model predictions (Fig. 2B), the different noise levels observed for this
24 reporter pair could be partially explained by distinct interaction strength distributions
25 of the competing RNA pool.

26 We performed a similar analysis for all the other pairs of reporters targeted by miRNAs
27 with $|\Delta R^M| < 0.1$. The competing RNAs were divided into a strong group and a weak

1 group with a ΔG_{total} threshold (7 kcal/mol), and the difference between the levels of
 2 competing RNAs in the strong group and the weak group was defined as the noise
 3 modulation capacity (MC, $\text{FPKM}_{\text{strong}} - \text{FPKM}_{\text{weak}}$) to roughly assess the integrated
 4 influence of competing RNAs on gene expression noise. Interestingly, the differences
 5 of noise between reporter pairs (ΔCV , $\text{CV}_{\text{miR-A}} - \text{CV}_{\text{miR-B}}$) with similar maximum
 6 repression strengths showed a moderate positive correlation with the differences of the
 7 miRNA noise modulation capacity (ΔMC , $\text{MC}_{\text{miR-A}} - \text{MC}_{\text{miR-B}}$) (Fig. 2E-F). This
 8 positive correlation was even more significant when using the miRmap score to define
 9 the interaction strength (miRmap score threshold = -0.05) (Fig. 2E and G). These
 10 observations supported the hypothesis that gene expression noise is buffered by weak
 11 competing RNAs.



12

1 Fig. 2. The influence of repression strength and competing RNAs on gene expression noise.
2 (A) Spearman correlation between repression strength (R) and noise (CV) among reporter systems
3 containing MREs with a single target of the top 20 most highly expressed miRNAs in HeLa cells at
4 different expression levels of EYFP. Solid lines and shading represent the mean \pm SD with three
5 independent replicates. Dashed lines represent the linear regression results of points.
6 (B) Simulation results of the influence of competing RNAs on gene expression levels and noise.
7 The simulation parameters are shown in Table S3.
8 (C) Competing RNA abundance associated with miR-19b-3p and miR-30a-5p under different ΔG_{total}
9 values.
10 (D) The difference between competing RNA abundance associated with miR-19b-3p and miR-30a-
11 5p under different ΔG_{total} values. The black line represents the smoothing of the abundance
12 distribution. The gray line represents the threshold of ΔG_{total} that divides the competing RNAs into
13 strong and weak groups.
14 (E) Spearman correlations between ΔCV and ΔMC divided by ΔG_{total} (dark blue line), between ΔCV
15 and ΔMC divided by the miRmap score (light blue line), and between ΔCV and $-\Delta R$ (gray line).
16 Solid and hollow points represent the significance of the correlation coefficients.
17 (F-G) Spearman correlations between ΔCV and ΔMC divided by the ΔG_{total} threshold (F) and
18 between ΔCV and ΔMC divided by the miRmap score threshold (G) at the EYFP expression level
19 of approximately $10^{3.5}$ a.u. Each point represents the mean \pm SD with three independent replicates.
20 Gray lines and shading represent the linear regression and the 0.95 confidence interval of the results.
21

22 **The composition of MREs influences miRNA-mediated noise modulation**

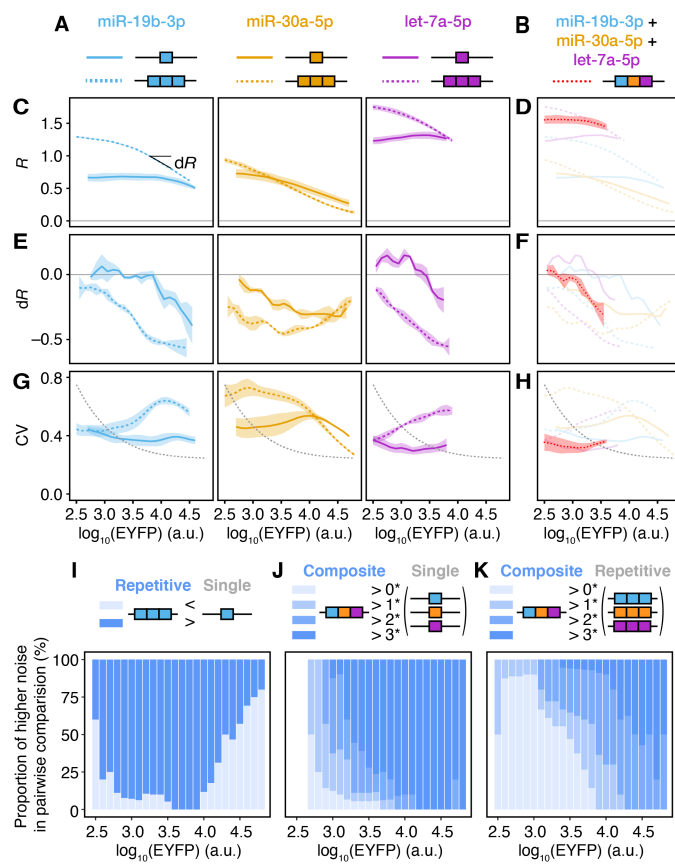
23 The 3'UTRs of both endogenous genes and genes included in synthetic circuits often
24 contain many miRNA binding sites (36, 37). Some 3'UTRs are targeted by the same
25 miRNA multiple times to enhance the repression strength of miRNAs (18). Some
26 3'UTRs are targeted by different miRNAs, constituting a complex regulatory network
27 controlling various biological processes robustly and precisely (38). Therefore, it is

1 necessary to investigate how the composition of MREs can influence gene expression
2 noise.

3 To investigate how multiple MREs of the same miRNA can modulate noise, we
4 constructed reporters that contain three perfect complementary tandem MREs for each
5 of the 20 miRNAs showing the highest expression in HeLa cells (Fig. 3A and Fig. S3).
6 Compared to reporters with a single MRE, reporters with triple MREs showed a greater
7 repression strength at low expression levels, but the repression strength decreased
8 markedly as expression increased (Fig. 3C), which is a consequence of the saturation
9 effect of miRNA regulation (34). The sensitivity of the strength of gene expression
10 repression (dR) around the threshold generated by saturation therefore increases in
11 reporters with triple MREs (Fig. 3E), which has been shown to increase gene expression
12 noise in previous studies (14, 26). Therefore, reporters with triple MREs showed
13 stronger noise reduction at low expression levels in comparison with those with a single
14 MRE but exhibited a remarkable increase in noise at high expression levels (Fig. 3I).
15 Furthermore, accompanied by the alteration of the threshold, the regime with maximum
16 sensitivity showed a shift to lower expression levels in triple-MRE reporters, causing
17 an increase in noise even at low expression levels, which counteracted the noise
18 reduction arising from the increased repression strength of triple MREs (Fig. 3G and I).
19 This phenomenon is consistent with previous work (25, 34).

20 We further used the reporter systems to assess the modulation pattern of MREs
21 composed of targets of different miRNAs. Each composite MRE is composed of three
22 perfectly complementary MREs that are targeted by miRNAs with adjacent expression
23 level ranks in HeLa cells. The top 20 most highly expressed miRNAs in HeLa cells
24 were selected, and they constituted 18 sequential composite targets. Interestingly, the
25 composite MREs exhibited distinct noise modulation patterns compared to repetitive
26 MREs and a single MRE (Fig. 3B, S4, and S5). In comparison with reporters with a
27 single MRE, reporters with composite MREs showed higher miRNA-mediated

1 repression strength and thus lower noise at low expression levels (Fig. 3D, H, and J).
 2 Additionally, the composite MREs could lead to greater saturation (Fig. 3F), thus
 3 increasing noise at very high expression levels (Fig. 3H, J, and S4). Compared with
 4 triple MREs, the composite MREs showed similar repression levels but a higher
 5 saturation threshold, leading to a wide range of noise reduction levels compared with
 6 repetitive MREs except in the case of extremely high expression levels (Fig. 3H and K
 7 and S5).



8
 9 Fig. 3. The influence of MRE composition on gene expression noise.
 10 (A-B) Schematic diagrams of a single MRE (A), triple repetitive MREs (A), and composite MREs
 11 (B).
 12 (C-H) Repression strength (C-D), saturation (E-F, the difference of repression strength) and noise
 13 (G-H) of reporters with a single MRE (colored solid lines), triple MREs (colored dashed lines),
 14 and composite MREs (red dotted lines). Lines and shading represent the mean \pm SD with three
 15 independent replicates. Gray lines represent reporters without the regulation of miRNAs.

1 (*I-K*) Comparison of noise (*I*) between the reporter with triple MREs and the reporter with the
2 corresponding single MRE, (*J*) between the reporter with composite MREs and all three reporters
3 with the corresponding single MRE, and (*K*) between the reporter with composite MREs and all
4 three reporters with the corresponding triple MREs. Only EYFP expression levels measured in \geq
5 five comparison groups are shown.

6

7 **MiRNA-mediated noise modulation could enhance state transition and improve** 8 **the accuracy of synthetic cell-type classifiers**

9 miRNAs have been widely employed in synthetic gene circuits as input signals to
10 classify cells of different types or in different states (39–44). Previous studies have
11 shown that gene expression noise can impact the performance of synthetic gene circuits
12 (3, 14), so it is reasonable to hypothesize that the ability of miRNAs to control gene
13 expression noise could further modulate the behaviors of gene circuits with miRNAs
14 as inputs. Here, we used a well-established miRNA-mediated TALER circuit that
15 behaves as a cell-type classifier (42) (Fig. 4A and S6A) to investigate whether miRNA-
16 mediated noise modulation can affect the classification accuracy of the circuit.

17 As shown in Figure 4A and S6A, the TALER switch was composed of two TALER
18 genes that could repress the transcription of each other, forming a closed-loop (CL)
19 topology. The TALER genes were fused with EYFP or mKate2 so that their expression
20 levels were reflected by the intensity of these fluorescent proteins. The expression of
21 both TALERS was driven by the transcription activator Gal4VP16 fused with TagBFP.
22 We selected the top eight most highly expressed miRNAs in HeLa cells and cloned one
23 perfectly complementary MRE or triple tandem perfectly complementary MREs for
24 each of them to the 3'UTR of EYFP-TALER. To exclude the influence of the
25 transfection efficiency on EYFP and mKate2 intensity, we binned cells according to
26 their TagBFP intensity and chose cells with TagBFP intensity between $10^{4.3}$ and $10^{4.4}$
27 a.u. for further analysis. The results for other bins exhibited similar trends and are

1 shown in supplementary figure S7.

2 Previous studies (42) have shown that CL switches without miRNA regulation exhibit
3 a state with moderate levels of both EYFP and mKate2. When the expression of EYFP
4 is repressed by miRNA, CL switches will transition to a low-EYFP, high-mKate2 state.
5 Cell state transitions were successfully observed in this study, but the extent of the
6 transition was quite different across these CL switches with different MREs (Fig. 4C).
7 Some CL switches exhibited an approximately complete transition to the low-EYFP,
8 high-mKate2 state, while others exhibited intermediate states. The CL TALER switches
9 could be used to classify different cell types or states employing different miRNAs as
10 input (42, 45), and an incomplete transition will decrease the classification accuracy
11 between the circuits with and without the inputs (Fig. 4C). We depicted the
12 classification accuracy in a receiver operating characteristic (ROC) curve and
13 quantified the accuracy by using the area under the ROC curve (AUC) (Fig. 4D).
14 Furthermore, to determine the repression-strength-independent influence of noise
15 modulation mediated by miRNAs on the performance of CL switches, we also
16 quantified the repression strength of each MRE by using an open-loop (OL) TALER
17 circuit, the only difference of which in comparison with the CL switch was that mKate2-
18 TALER could not repress the expression of EYFP-TALER (Fig. 4B and S6B).

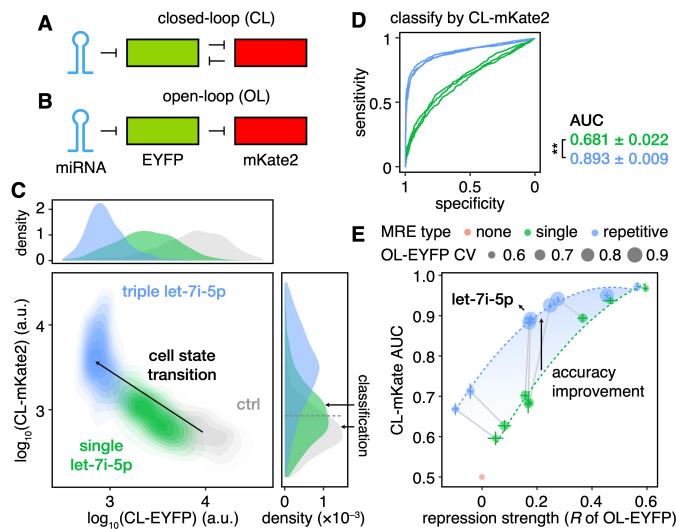
19 As shown in Figure 4E, the classification accuracies were positively correlated with the
20 repression strength. However, circuits with MREs sharing similar repression strengths
21 in OL circuits could exhibit distinct AUCs in CL switches. In particular, CL switches
22 with triple tandem MREs (blue points) showed higher classification accuracies than
23 those with a single MRE (green points), which was consistent across all TagBFP
24 intensity bins (Fig. S7). For instance, single let-7i-5p MRE and triple let-7i-5p MREs
25 could lead to similar repression strengths in OL circuits (Fig. 4E and S8A), but only the
26 CL switch with triple let-7i-5p MREs exhibited a near-complete state transition (Fig.
27 4C) in comparison with the CL switch with single let-7i-5p MRE, leading to higher

1 classification accuracy (Fig. 4D-E).

2 To understand the mechanism of such phenomena, we examined the behavior of OL
3 circuits with these MREs. The OL circuits can be regarded as a signal transduction
4 cascade in which the signal of miRNA propagates to mKate2-TALER via EYFP-
5 TALER. We found that although similar repression strengths in the first step (EYFP)
6 were exerted, circuits with triple MREs could induce a greater expression increase in
7 the second step (mKate2) (Fig. S8B). For example, although the OL circuit with triple
8 let-7i-5p MREs exhibited the same EYFP level as that with a single let-7i-5p MRE, the
9 former circuit showed a significantly higher mKate2 level than the latter (Fig. S8A).
10 The experimental results of the dual-fluorescent reporter system showed that triple
11 MREs could introduce higher noise at low and intermediate expression levels in
12 comparison with a single MRE, independent of repression strength (Fig. 3). Therefore,
13 we speculated that the miRNA-mediated modulation of noise may affect the signal
14 transduction efficiency of the OL circuits, and it may further influence the classification
15 accuracy of CL switches.

16 We performed Monte Carlo simulations (46) to investigate the impact of noise. In OL
17 circuits, the results showed that when mean EYFP levels were equal, higher EYFP noise
18 could lead to a higher mKate2 level, resulting from the nonlinear relationship between
19 EYFP and mKate2 (Fig. S9A-B). In CL switches, the increase in the mKate2 level
20 caused by higher EYFP noise could in turn suppress the expression of EYFP, thus
21 bringing about a significant change of the distribution to a lower-EYFP and higher-
22 mKate2 situation (Fig. S9D-F). Besides, in CL switches, where the expression of EYFP
23 was repressed by mKate2, the stronger saturation effects of repetitive MREs in
24 comparison with the single MRE (Fig. 3E) could lead to a more remarkable increase of
25 repression strength in CL switches (Fig. S9C), which resulted in the alteration of the
26 steady state to a low-EYFP and high-mKate2 state (Fig. S9D-E). Therefore, the
27 alteration of repression strength caused by saturation promoted the cell state transitions

1 in CL switches, and the high expression noise modulated by MREs further enhanced
 2 the cell state transitions (Fig. S9E and F), both of which upheld the improvement of
 3 classification accuracy (Fig. S9G). The results suggested that detailed characteristics of
 4 miRNA regulation should be taken into account in the design of synthetic circuits with
 5 miRNAs.



6
 7 Fig. 4. miRNAs can regulate the behavior of TALER switches by modulating gene expression
 8 noise.

9 (A) Schematic diagrams of closed-loop (CL) TALER switches.

10 (B) Schematic diagrams of open-loop (OL) TALER circuits.

11 (C) Joint and marginal distribution of EYFP and mKate2 in CL switches.

12 (D) ROC curves obtained when classifying cells by mKate2 in CL switches. Student's *t*-tests were
 13 performed between the AUCs of two groups, and the significance levels are indicated by **: $p <$
 14 0.01.

15 (E) The relationship between the repression strength of MREs in OL circuits and the AUCs
 16 classified by mKate2 in CL switches. The size of the point represents the noise level (CV) of
 17 EYFP mediated by the MRE in OL circuits. Dashed curves represent the loess regression of the
 18 points. Each point represents the mean \pm SD with three independent replicates. Points that
 19 represent reporters with single MRE or triple MREs of the same miRNA are connected by gray
 20 lines.

1

2 **Discussion**

3 We applied mathematical modeling and a dual-fluorescent reporter system to
4 investigate how competing RNAs and miRNA binding sites of genes influence the
5 expression noise of genes at different expression levels. We showed that genes targeted
6 by miRNAs with weak competing RNAs tend to exhibit lower noise than those without
7 MREs or those targeted by miRNAs with strong competing RNAs at a wide range of
8 gene expression levels. In addition, repetitive MREs of the same miRNA can reduce
9 noise at low expression levels but increase gene expression noise at high expression
10 levels compared to a single MRE, while composite MREs composed of targets for
11 different miRNAs can maintain low-expression noise reduction but reduce the increase
12 of high-expression noise. We showed that the proper choice of miRNAs and
13 corresponding MREs to modulate gene expression noise could significantly enhance
14 cell state transition and improve the performance of synthetic gene circuits for cell
15 classification.

16 Each miRNA has tens or hundreds of targets, but most of them are weakly repressed,
17 raising questions about the function of the widespread weak interactions between
18 miRNAs and their targets (29–31). A generally accepted hypothesis posited that
19 miRNAs usually make fine-scale adjustments to most of their targets (17, 19, 28). An
20 alternative proposed view is that a large proportion of miRNA targets are competitive
21 inhibitors of miRNAs. Moderate repression of these targets might not lead to
22 consequences at the physiological level (28) but may function to titrate miRNA activity,
23 instead of being regulated by miRNAs (17). Our results suggested that widespread weak
24 interactions might act as buffers to reduce gene expression noise (Fig. 2) and thus confer
25 robustness to gene regulatory networks, similar to previous theoretical analysis (47, 48)
26 and our observations at the mRNA level (27).

1 It is noteworthy that current algorithms for predicting miRNA targets, such as miRmap
2 (35, 49), TargetScan (50), and PITA (51), were designed to discover targets that are
3 thought to be repressed by corresponding miRNAs with high confidence. To reduce the
4 false-positive rate, these algorithms usually ignore weak or nonconserved targets.
5 However, it has been suggested that the number of these weak targets that cannot be
6 predicted by current algorithms is quite large and that they might play important roles
7 in the regulation of gene expression by miRNAs (52). According to our computational
8 simulation results, these widespread weak targets can buffer gene expression noise.
9 Therefore, if algorithms for predicting these weak targets can be developed in the future,
10 we could better understand the modulation of gene expression noise by miRNAs and
11 employ the results of this study to explain the function of endogenous miRNAs in
12 biological processes or modulate the performance of synthetic gene circuits.

13 In synthetic gene circuits with miRNAs as inputs, MREs are often designed as tandem
14 repeats of the same miRNA instead of a single MRE of the miRNA (39, 42, 53). We
15 have shown that genes with repetitive MREs may exhibit higher noise levels at high
16 expression levels or even globally than those with a single MRE, demonstrating that
17 the composition of MREs can strongly influence gene expression noise. In addition, as
18 shown in the TALER-based cell-type classifiers, switches with repetitive MREs
19 exhibited better classification accuracies than those with a single MRE when subjected
20 to similar repression strengths measured in OL circuits. The results indicated that during
21 the design of MREs in synthetic gene circuits, it is necessary to consider not only the
22 repression strengths measured in some certain conditions, but also miRNA-mediated
23 modulations of noise and saturation as well as the intricate behaviors of the modulations
24 in gene regulatory networks.

25 The engineering of large-scale synthetic gene circuits is limited by the poor stability of
26 the complex system, which is usually caused by noise in gene expression. Previous
27 studies have revealed several strategies for modulating gene expression noise without

1 changing the mean expression levels, including the mutation of TATA boxes (2, 54), the
2 regulation of transcriptional rates and translational rates at the same time (3), the
3 alteration of epigenetics (55) and the arrangement of two transcriptional regulators (56).
4 Our investigation of the influence of miRNA properties on gene expression noise might
5 provide a new tool for modulating noise in synthetic gene circuits and thus regulating
6 their behaviors.

7 In summary, we performed an elaborate analysis of how competing RNAs and the
8 composition of MREs influence gene expression noise and how such modulation could
9 further impact the performance of synthetic gene circuits. The results provided an
10 explanation for the function of the widespread weak interactions between miRNAs and
11 their targets and presented guidelines for the design of miRNA binding sites in synthetic
12 gene circuits to better employ miRNAs as endogenous signals.

13

14 **Materials and Methods**

15 **Reagents and enzymes**

16 Polynucleotide kinase (PNK), ATP, T4 ligase, and all restriction endonucleases were
17 purchased from New England Biolabs. Oligonucleotides were synthesized by Genewiz.
18 Doxycycline (Dox) was purchased from Clontech.

19 **Construction of dual-fluorescent reporter systems and TALER switches**

20 The sequences of the single MREs are listed in Table S1. The sequences of the triple
21 MREs consisted of three tandem single MRE sequences without gaps. The sequences
22 of the composite MREs were joint by single MRE sequences of three miRNAs with
23 adjacent ranks of expression levels without gaps. The MREs were synthesized as
24 oligonucleotides, which were annealed and then phosphorylated using PNK and ATP

1 for ligation. The MREs were then inserted into the 3'UTR of EYFP in the dual-
2 fluorescent reporter system via the SpeI and HindIII digestion sites with T4 ligase.

3 The TALER-based switches were modified from circuits described in a previous study
4 (42). The closed-loop (CL) switch (Fig. S6A) was composed of three plasmids. The
5 constitutively expressed transcription activator Gal4VP16, which was fused with
6 TagBFP via a self-cleaving 2A linker (Gal4VP16-2A-TagBFP, or Gal4VP16-TagBFP
7 in short) (57), drove the expression of EYFP-2A-TALER9 and mKate2-2A-TALER14.
8 The promoter of EYFP-TALER9 was flanked with four TALER14 binding sites (T14),
9 and the promoter of mKate2-TALER14 was flanked with four TALER9 binding sites
10 (T9). Therefore, EYFP-TALER9 and mKate2-TALER14 exerted mutual expression
11 inhibition against each other. The MREs were inserted into the 3'UTR of EYFP-
12 TALER9 via the SpeI and MluI digestion sites with T4 ligase. Compared with the CL
13 switch, the only difference in the open-loop (OL) circuit was that mKate2-TALER14
14 was replaced by mKate2-TALER10 so that the expression of mKate2-TALER10 could
15 not inhibit the expression of EYFP-TALER9 (Fig. S6B).

16 **Cell culture, transient transfection and flow cytometry**

17 HeLa cells (originally obtained from ATCC) were grown in DMEM with 4.5 g/L
18 glucose (Gibco) supplemented with 10% FBS (Gibco) at 37 °C and 5% CO₂. On the
19 day before transfection, approximately 1.6×10^5 HeLa cells were plated in 12-well plates.
20 Lipofectamine LTX (Thermo Fisher) was used for transfection according to the
21 manufacturer's protocol. For the observation of dual-fluorescent reporter systems,
22 transfection with 40 ng of the plasmids carrying the dual-fluorescent reporter, 40 ng of
23 the plasmids carrying the reverse tetracycline-controlled transactivator (rtTA) gene, and
24 420 ng of pDT004, a plasmid with no protein-coding sequences (42), was performed in
25 the wells of a 12-well plate. For the observation of TALER switches, the transfection
26 of 100 ng of the plasmids carrying Gal4VP16-TagBFP, 100 ng of the plasmids carrying
27 EYFP-TALER9-MRE, and 100 ng of the plasmids carrying mKate2-TALER10 (for OL)

1 or mKate2-TALER14 (for CL) in the wells of a 12-well plate. On the day of transfection
2 and one day after transfection, the medium was refreshed with DMEM. For the dual-
3 fluorescent reporters, we supplemented DMEM with 1 $\mu\text{g/ml}$ Dox to induce their
4 expression. Cells were harvested 48 h after transfection and centrifuged at 500 g for 3
5 min at room temperature. Then, the cells were washed with PBS once and resuspended
6 in PBS. Flow cytometry was conducted using Fortessa flow analyzers (BD Biosciences)
7 with the settings listed in Table S2. For the dual-fluorescent reporter systems,
8 approximately 3×10^4 mKate2-positive cells were collected. For the TALER switches,
9 approximately 5×10^4 TagBFP-positive cells were collected.

10 **High-throughput sequencing of HeLa cells**

11 The miRNA-seq of HeLa cells was conducted on the HiSeq 2500 platform (Illumina)
12 and analyzed by using miRDeep2 (v 0.1.2). The RNA-seq of HeLa cells was conducted
13 on the NovaSeq 6000 platform (Illumina) and analyzed by using TopHat (v 2.1.1) and
14 HTSeq (v 0.6.1).

15 **Flow cytometry data processing**

16 All data processing and analysis described below were performed by using R v3.6.1.
17 For the dual-fluorescent reporter system used to measure gene expression noise, the
18 data were processed as previously described with some modifications (20), as follows.
19 Cells were binned according to the mKate2 intensity (bin width 0.2 in \log_{10} space).
20 Cells with mKate2 intensity of less than 10^2 were considered to be untransfected cells
21 and were thus removed. In each bin, cells above the 0.05 quantile and below the 0.95
22 quantile of the EYFP intensity distribution were selected. Three independent biological
23 replicates were performed for each reporter. The noise of reporters without MREs was
24 fitted using the method described in Ref. (20).

25 For the data of TALER circuits, the cells were binned according to the TagBFP intensity

1 (bin width 0.1 in log₁₀ space) to control the transfection efficiency. Cell type
2 classification was performed between the CL switches with MREs and without MREs
3 in the same replicate.

4 The repression strength, R , of each miRNA was calculated as the difference between
5 the logarithmic mean value of EYFP without miRNA regulation (μ_0) and with miRNA
6 regulation (μ) at the same transcriptional level (in the same mKate2 bin for the dual-
7 fluorescent reporter system or the same TagBFP bin for the OL TALER circuits): $R =$
8 $\log_{10}(\mu_0) - \log_{10}(\mu)$.

9 For the dual-fluorescent reporter system, R and CV were interpolated in the space of
10 the EYFP mean expression level. The repression strength at the lowest EYFP
11 expression level was regarded as the maximum repression strength, R^M . miRNA pairs
12 with similar R^M ($|R^M_{\text{miR-A}} - R^M_{\text{miR-B}}| < 0.1$) values were considered to be pairs of
13 miRNAs with the same repression strength for further analysis in Fig. 2E-G.

14 **Characterization of competing RNAs**

15 We calculated competing RNA abundance from the RNA-seq data of HeLa cells and
16 the miRNA target predictions for humans by using miRmap (release mirmap201301e).
17 For the analysis based on ΔG_{total} , all transcripts with $\Delta G_{\text{total}} < 7$ kcal/mol were regarded
18 as strong competing RNAs; otherwise, they were regarded as weak competing RNAs.
19 The total abundance (FPKM) of the strong and weak competing RNAs was used to
20 define the noise modulation capacity (MC): $\text{MC} = \text{FPKM}_{\text{strong}} - \text{FPKM}_{\text{weak}}$. For analysis
21 based on the miRmap score, all transcripts with a miRmap score < -0.05 were regarded
22 as strong competing RNAs.

23 **Mathematical modeling of gene expression noise**

24 The mathematical model and parameter settings for simulating the noise modulation of
25 competing RNAs were adopted from our previous work (26). The model is briefly

1 described using ordinary differential equations (ODEs) as follows:

$$2 \quad \frac{dR^F}{dt} = k_R - g_R R^F - (k_{1+} T_1^F + k_{2+} T_2^F) R^F + k_{1-} T_1^C + k_{2-} T_2^C + (1 - \alpha_1) g_1 T_1^C + (1 - \alpha_2) g_2 T_2^C$$

$$4 \quad \frac{dT_1^F}{dt} = k_{T1} - g_{T1} T_1^F - k_{1+} T_1^F R^F + k_{1-} T_1^C$$

$$5 \quad \frac{dT_1^C}{dt} = k_{1+} T_1^F R^F - k_{1-} T_1^C - g_1 T_1^C$$

$$6 \quad \frac{dT_2^F}{dt} = k_{T2} - g_{T2} T_2^F - k_{2+} T_2^F R^F + k_{2-} T_2^C$$

$$7 \quad \frac{dT_2^C}{dt} = k_{2+} T_2^F R^F - k_{2-} T_2^C - g_2 T_2^C$$

$$8 \quad \frac{dP_1}{dt} = k_{P1} T_1^F - g_{P1} P_1$$

9 Where R^F denotes the concentration of free miRNA; T_i^F denotes the concentration of
 10 free RNA # i ; T_i^C denotes the concentration of the complex of miRNA and RNA # i ; P_1
 11 denotes the protein of RNA #1. In this model, RNA #1 represents the RNA transcribed
 12 from the observed gene, and RNA #2 represents the competing RNA. k_{Ti} is the
 13 transcription rate of RNA # i . g_{Ti} is the degradation rate of RNA # i . RNA # i and the
 14 miRNA form a complex at a rate of k_{i+} , and the complex dissociates at a rate of k_{i-} and
 15 degrade at a rate of g_i . When complex # i degrades, miRNAs on the complex degrades
 16 with a probability of α_i . The production and degradation rate of the protein of RNA #1
 17 are k_{P1} and g_{P1} respectively. The transcription and degradation rate of the miRNA are
 18 k_R and g_R respectively. The noise levels of all the molecular species are calculated using
 19 fluctuation-dissipation theorem as in Ref. (26). The parameters for Fig. 2B are shown
 20 in Table S3.

21 **Stochastic simulation of TALER circuits**

1 To model how the noise of EYFP-TALER influences the level of mKate2-TALER, we
 2 conducted a stochastic simulation using the Gillespie algorithm (46). The EYFP-
 3 TALER was denoted as E , and the mKate2-TALER was denoted as K . The transcription
 4 of K mRNAs (T_K) was repressed by E proteins (P_E) in both OL and CL circuits, while
 5 the transcription of E mRNAs (T_E) was repressed by K proteins (P_K) only in CL
 6 switches. T_E and T_K transcribes at a rate of k_{TE} and k_{TK} respectively without repression.
 7 The repressions of P_K for T_E and P_E for T_K follow the Hill's function. For the repression
 8 of P_E for T_K , K_E denotes the number of P_E that gives 50% repression of T_K , and m
 9 denotes the Hill coefficient of this reaction. For the repression of P_K for T_E , which only
 10 exists in CL switches, K_K denotes the number of P_K that gives 50% repression of T_E ,
 11 and n denotes the Hill coefficient of this reaction. The values of Hill coefficients were
 12 adopted from Ref (42). g_{TE} , g_{TK} , g_{PE} and g_{PK} denote the degradation rate of T_E , T_K , P_E
 13 and P_K respectively. The deterministic model of OL circuits is described in the
 14 following ODEs:

$$15 \quad \frac{dT_E}{dt} = k_{TE} - g_{TE}T_E$$

$$16 \quad \frac{dP_E}{dt} = k_{PE}T_E - g_{PE}P_E$$

$$17 \quad \frac{dT_K}{dt} = k_{TK} \frac{K_E^m}{K_E^m + P_E^m} - g_{TK}T_K$$

$$18 \quad \frac{dP_K}{dt} = k_{PK}T_K - g_{PK}P_K$$

19 In CL switches, the first equation is replaced by

$$20 \quad \frac{dT_E}{dt} = k_{TE} \frac{K_K^n}{K_K^n + P_K^n} - g_{TE}T_E$$

21 Two major factors of miRNA regulation, repression strength and gene expression noise,
 22 were simulated separately. We defined k_{TE0} and g_{TE0} as the production rate and

1 degradation rate of T_E in the condition without the regulation of miRNA. Furthermore,
2 we defined the relative repression rate R and the turnover rate t for a certain condition,
3 where

$$4 \quad k_{TE} = tk_{TE0}$$

$$5 \quad g_{TE} = tRg_{TE0}$$

6 The relative repression rate R represents the condition with or without the regulation of
7 miRNA and the difference of repression strengths in CL switches. The turnover rate t
8 represents different expression noise of EYFP-TALER. A high turnover rate indicates
9 low noise, and a low turnover rate indicates high noise. The parameters are listed in
10 Table S4.

11 For simulation using Gillespie algorithm, there are 8 reactions total: the production and
12 degradation of T_E , T_K , P_E , P_K respectively. Their propensity functions in the Gillespie
13 algorithm are the same with the coefficients in the ODEs. We simulated 100 trajectories
14 for each parameter setting. After the fluctuation reached an approximately steady state
15 ($t = 10000$ s), a total of 400 points were sampled per 100 seconds from every trajectory
16 for plotting Fig. S9A and S9D. The mean values of EYFP and mKate2 from 10000 s to
17 50000 s of all trajectories were used to perform the Mann–Whitney U test in Fig. S9B
18 and S9F.

19

20 **Acknowledgments**

21 This work has been supported by the National Natural Science Foundation of China
22 (No. 61773230, 61721003).

23 **Author Contributions**

1 X.W., L.W. and S.L. designed the research; L.W. and S.L. performed the experiments
2 and analyzed the data; L.W., S.L. and T.H. built mathematical models and performed
3 the simulations; L.W. and S.L. wrote the manuscript, with all authors contributing to
4 the writing and providing feedback.

5 **Competing interests**

6 The authors declare that they have no competing interests.

7

8 **References**

- 9 1. M. B. Elowitz, Stochastic Gene Expression in a Single Cell. *Science* **297**, 1183–
10 1186 (2002).
- 11 2. W. J. Blake, *et al.*, Phenotypic Consequences of Promoter-Mediated
12 Transcriptional Noise. *Mol. Cell* **24**, 853–865 (2006).
- 13 3. H. Maamar, A. Raj, D. Dubnau, Noise in Gene Expression Determines Cell Fate
14 in *Bacillus subtilis*. *Science* **317**, 526–529 (2007).
- 15 4. G. M. Suel, R. P. Kulkarni, J. Dworkin, J. Garcia-Ojalvo, M. B. Elowitz,
16 Tunability and Noise Dependence in Differentiation Dynamics. *Science* **315**, 1716–
17 1719 (2007).
- 18 5. T. Çağatay, M. Turcotte, M. B. Elowitz, J. Garcia-Ojalvo, G. M. Süel,
19 Architecture-Dependent Noise Discriminates Functionally Analogous Differentiation
20 Circuits. *Cell* **139**, 512–522 (2009).
- 21 6. H. H. Chang, M. Hemberg, M. Barahona, D. E. Ingber, S. Huang, Transcriptome-
22 wide noise controls lineage choice in mammalian progenitor cells. *Nature* **453**, 544–
23 547 (2008).
- 24 7. T. Kalmar, *et al.*, Regulated Fluctuations in Nanog Expression Mediate Cell Fate
25 Decisions in Embryonic Stem Cells. *PLoS Biol.* **7**, e1000149 (2009).
- 26 8. J. Hanna, *et al.*, Direct cell reprogramming is a stochastic process amenable to
27 acceleration. *Nature* **462**, 595–601 (2009).
- 28 9. S. L. Spencer, S. Gaudet, J. G. Albeck, J. M. Burke, P. K. Sorger, Non-genetic
29 origins of cell-to-cell variability in TRAIL-induced apoptosis. *Nature* **459**, 428–432
30 (2009).
- 31 10. P. B. Gupta, *et al.*, Stochastic State Transitions Give Rise to Phenotypic
32 Equilibrium in Populations of Cancer Cells. *Cell* **146**, 633–644 (2011).
- 33 11. A. Brock, H. Chang, S. Huang, Non-genetic heterogeneity — a mutation-
34 independent driving force for the somatic evolution of tumours. *Nat. Rev. Genet.* **10**,

- 1 336–342 (2009).
- 2 12. S. Hooshangi, S. Thiberge, R. Weiss, Ultrasensitivity and noise propagation in a
3 synthetic transcriptional cascade. *Proc. Natl. Acad. Sci.* **102**, 3581–3586 (2005).
- 4 13. J. M. Pedraza, Noise Propagation in Gene Networks. *Science* **307**, 1965–1969
5 (2005).
- 6 14. W. J. Blake, M. Kærn, C. R. Cantor, J. J. Collins, Noise in eukaryotic gene
7 expression. *Nature* **422**, 633–637 (2003).
- 8 15. M. Kærn, T. C. Elston, W. J. Blake, J. J. Collins, Stochasticity in gene
9 expression: from theories to phenotypes. *Nat. Rev. Genet.* **6**, 451–464 (2005).
- 10 16. A. Eldar, M. B. Elowitz, Functional roles for noise in genetic circuits. *Nature*
11 **467**, 167–173 (2010).
- 12 17. S. L. Ameres, P. D. Zamore, Diversifying microRNA sequence and function. *Nat.*
13 *Rev. Mol. Cell Biol.* **14**, 475–488 (2013).
- 14 18. D. P. Bartel, Metazoan MicroRNAs. *Cell* **173**, 20–51 (2018).
- 15 19. D. P. Bartel, C.-Z. Chen, Micromanagers of gene expression: the potentially
16 widespread influence of metazoan microRNAs. 5.
- 17 20. J. M. Schmiedel, *et al.*, MicroRNA control of protein expression noise. *Science*
18 **348**, 128–132 (2015).
- 19 21. M. S. Ebert, P. A. Sharp, Roles for MicroRNAs in Conferring Robustness to
20 Biological Processes. *Cell* **149**, 515–524 (2012).
- 21 22. D. M. Kasper, *et al.*, MicroRNAs Establish Uniform Traits during the
22 Architecture of Vertebrate Embryos. *Dev. Cell* **40**, 552–565.e5 (2017).
- 23 23. E. Ferro, C. Enrico Bena, S. Grigolon, C. Bosia, microRNA-mediated noise
24 processing in cells: A fight or a game? *Comput. Struct. Biotechnol. J.* **18**, 642–649
25 (2020).
- 26 24. J. Schmiedel, D. S. Marks, B. Lehner, N. Bluthgen, Noise control is a primary
27 function of microRNAs and post-transcriptional regulation. *Biorxiv* (2017).
- 28 25. C. Bosia, *et al.*, RNAs competing for microRNAs mutually influence their
29 fluctuations in a highly non-linear microRNA-dependent manner in single cells.
30 *Genome Biol.* **18** (2017).
- 31 26. L. Wei, *et al.*, Regulation by competition: a hidden layer of gene regulatory
32 network. *Quant. Biol.* **7**, 110–121 (2019).
- 33 27. T. Hu, *et al.*, Single cell transcriptomes reveal characteristics of miRNA in gene
34 expression noise reduction. *bioRxiv*, 465518 (2018).
- 35 28. H. Seitz, Redefining MicroRNA Targets. *Curr. Biol.* **19**, 870–873 (2009).
- 36 29. M. Selbach, *et al.*, Widespread changes in protein synthesis induced by
37 microRNAs. *Nature* **455**, 58–63 (2008).
- 38 30. D. Baek, *et al.*, The impact of microRNAs on protein output. *Nature* **455**, 64–71
39 (2008).
- 40 31. A. Grimson, *et al.*, MicroRNA Targeting Specificity in Mammals: Determinants
41 beyond Seed Pairing. *Mol. Cell* **27**, 91–105 (2007).
- 42 32. Y. Yuan, *et al.*, Model-guided quantitative analysis of microRNA-mediated
43 regulation on competing endogenous RNAs using a synthetic gene circuit. *Proc. Natl.*

- 1 *Acad. Sci.* **112**, 3158–3163 (2015).
- 2 33. J. Noorbakhsh, A. H. Lang, P. Mehta, Intrinsic Noise of microRNA-Regulated
- 3 Genes and the ceRNA Hypothesis. *PLoS ONE* **8**, e72676 (2013).
- 4 34. S. Mukherji, *et al.*, MicroRNAs can generate thresholds in target gene expression.
- 5 *Nat. Genet.* **43**, 854–859 (2011).
- 6 35. C. E. Vejnar, E. M. Zdobnov, miRmap: Comprehensive prediction of microRNA
- 7 target repression strength. *Nucleic Acids Res.* **40**, 11673–11683 (2012).
- 8 36. R. C. Friedman, K. K.-H. Farh, C. B. Burge, D. P. Bartel, Most mammalian
- 9 mRNAs are conserved targets of microRNAs. *Genome Res.* **19**, 92–105 (2008).
- 10 37. L. S. Hon, Z. Zhang, The roles of binding site arrangement and combinatorial
- 11 targeting in microRNA repression of gene expression. *Genome Biol.* **8**, R166 (2007).
- 12 38. Z. Liufu, *et al.*, Redundant and incoherent regulations of multiple phenotypes
- 13 suggest microRNAs' role in stability control. *Genome Res.* **27**, 1665–1673 (2017).
- 14 39. Z. Xie, L. Wroblewska, L. Prochazka, R. Weiss, Y. Benenson, Multi-Input
- 15 RNAi-Based Logic Circuit for Identification of Specific Cancer Cells. *Science* **333**,
- 16 1307–1311 (2011).
- 17 40. K. Miki, *et al.*, Efficient Detection and Purification of Cell Populations Using
- 18 Synthetic MicroRNA Switches. *Cell Stem Cell* **16**, 699–711 (2015).
- 19 41. B. D. Brown, *et al.*, Endogenous microRNA can be broadly exploited to regulate
- 20 transgene expression according to tissue, lineage and differentiation state. *Nat.*
- 21 *Biotechnol.* **25**, 1457–1467 (2007).
- 22 42. Y. Li, *et al.*, Modular construction of mammalian gene circuits using TALE
- 23 transcriptional repressors. *Nat. Chem. Biol.* **11**, 207–213 (2015).
- 24 43. M. K. Sayeg, *et al.*, Rationally Designed MicroRNA-Based Genetic Classifiers
- 25 Target Specific Neurons in the Brain. *ACS Synth. Biol.* **4**, 788–795 (2015).
- 26 44. H. Huang, *et al.*, Oncolytic adenovirus programmed by synthetic gene circuit for
- 27 cancer immunotherapy. *Nat. Commun.* **10**, 4801 (2019).
- 28 45. D. Ma, S. Peng, Z. Xie, Integration and exchange of split dCas9 domains for
- 29 transcriptional controls in mammalian cells. *Nat. Commun.* **7**, 13056 (2016).
- 30 46. D. T. Gillespie, The chemical Langevin equation. *J. Chem. Phys.* **113**, 297–306
- 31 (2000).
- 32 47. Y. Zhao, X. Shen, T. Tang, C.-I. Wu, Weak Regulation of Many Targets Is
- 33 Cumulatively Powerful—An Evolutionary Perspective on microRNA Functionality.
- 34 *Mol. Biol. Evol.* **34**, 3041–3046 (2017).
- 35 48. Y. Zhao, *et al.*, Regulation of Large Number of Weak Targets—New Insights
- 36 from Twin-microRNAs. *Genome Biol. Evol.* **10**, 1255–1264 (2018).
- 37 49. C. E. Vejnar, M. Blum, E. M. Zdobnov, miRmap web: comprehensive microRNA
- 38 target prediction online. *Nucleic Acids Res.* **41**, W165–W168 (2013).
- 39 50. V. Agarwal, G. W. Bell, J.-W. Nam, D. P. Bartel, Predicting effective microRNA
- 40 target sites in mammalian mRNAs. *eLife* **4** (2015).
- 41 51. M. Kertesz, N. Iovino, U. Unnerstall, U. Gaul, E. Segal, The role of site
- 42 accessibility in microRNA target recognition. *Nat. Genet.* **39**, 1278–1284 (2007).
- 43 52. R. Denzler, *et al.*, Impact of MicroRNA Levels, Target-Site Complementarity,

- 1 and Cooperativity on Competing Endogenous RNA-Regulated Gene Expression. *Mol.*
2 *Cell* **64**, 565–579 (2016).
- 3 53. J. J. Gam, J. Babb, R. Weiss, A mixed antagonistic/synergistic miRNA repression
4 model enables accurate predictions of multi-input miRNA sensor activity. *Nat.*
5 *Commun.* **9** (2018).
- 6 54. K. F. Murphy, R. M. Adams, X. Wang, G. Balázsi, J. J. Collins, Tuning and
7 controlling gene expression noise in synthetic gene networks. *Nucleic Acids Res.* **38**,
8 2712–2726 (2010).
- 9 55. R. D. Dar, N. N. Hosmane, M. R. Arkin, R. F. Siliciano, L. S. Weinberger,
10 Screening for noise in gene expression identifies drug synergies. *Science* **344**, 1392–
11 1396 (2014).
- 12 56. A. Aranda-Díaz, K. Mace, I. Zuleta, P. Harrigan, H. El-Samad, Robust Synthetic
13 Circuits for Two-Dimensional Control of Gene Expression in Yeast. *ACS Synth. Biol.*
14 **6**, 545–554 (2017).
- 15 57. A. L. Szymczak, *et al.*, Correction of multi-gene deficiency in vivo using a single
16 “self-cleaving” 2A peptide–based retroviral vector. *Nat. Biotechnol.* **22**, 589–594
17 (2004).
- 18
- 19